جامعة عين شمس
Faculty of Women for, Arts, Science, and Education
Scientific Publishing Unit

Journal of Scientific Research in Science

Basic Sciences

Volume 39, Issue 1, 2022

ISSN 2356-8372 (Online) \ ISSN 2356-8364 (print)

Journal of Scientific Research in Science 2022, 39, (1): 61-82

Contents lists available at EKB

Journal of Scientific Research in Science

Journal homepage: https://jsrs.journals.ekb.eg/

Energy staggering in superdeformed bands for isodiaphere nuclei in A ~ 40-60 mass region

Eman R. Abo Elyazeed[1,*], Hager H. Soudii[1], D. A. Elrayen[1], Hayam Yassin[1]

[1] Physics Department, Faculty of Women for Arts, Science and Education, Ain Shams University, Cairo, Egypt.

Abstract

The properties of superdeformed (SD) bands of isodiaphere nuclei (^{40}Ca,^{58}Cu,^{60}Zn) have been studied in the scope of four and five parameters' formulas of the Bohr-Mottelson collective model. The unknown parameters are obtained by fitting the experimental measurements of the gamma-ray transition energies using MATLAB software. The rotational frequency $\hbar\omega$, the kinematic $J^{(1)}$, and dynamic $J^{(2)}$ moments of inertia are determined by using the best fitted parameters. The obtained γ-ray transition energies $E\gamma$ are in good agreement with the experimental measurements. Also, the theoretical results of the kinematic $J^{(1)}$, and dynamic $J^{(2)}$ moments of inertia using both formulas agree well with the experimental data. The staggering $\Delta I = 2$ phenomenon is represented by using various order derivatives of γ-ray transition energies E_γ with respect to spin angular momentum *I*. We conclude that the five parameters formula of Bohr-Mottelson collective model successes in interpreting the appeared pairing correlations in the experimental measurements for the studied nuclei.

Keywords:

Superdeformed nuclei, Nuclear energy levels, Energy staggering, moment of inertia

1. Introduction

One of the most interesting topics in nuclear structure physics is the discovery of superdeformed (SD) bands in traditional mass regions such as A ~ 190 [1,2], 150 [3], 130 [4, 5], 80, [6 - 11] and 60 [12 - 14]. Additionally, SD bands were discovered in medium-light nuclei $A <$ 60 like ^{56}Ni [15], ^{36}Ar [16,17] and ^{40}Ca [18]. The levels of double magic nucleus ^{40}Ca were described as a mixture of spherical shell model and rotational model [19, 20]. Also, Svensson et al. observed the SD bands in ^{60}Zn nucleus [13].

***Corresponding author:** Eman R. Abo Elyazeed, Physics Department, Faculty of Women for Arts, Science and Education, Ain-Shams University, Cairo, Egypt.

E-mail: eman.reda@women.asu.edu.eg, hiam_hussien@women.asu.edu.eg

https://doi.org/10.21608/JSRS.2022.275774

(Received 08 September 2022, revised 30 November 2022, accepted 01 December 2022)

The behavior of dynamic moment of inertia $J^{(2)}$ is being used as a tool to distinguish between the SD bands in various mass regions [21]. In region A~150, the characteristic of intruder orbital configuration was demonstrated by different behavior of $J^{(2)}$ from the one in A ~190 region where $J^{(2)}$ increased with the increase in the rotational frequency $\hbar\omega$ [22]. The unknown bandhead spin angular momentum is the main problem in SD bands till now. Various theoretical models have proposed to guess the spin assignments of SD bands [22 - 33]. Also, the excitation energies levels were unmeasured to some SD bands [22]. Furthermore, lower mass *A* region has an importance than the higher one because of the finite number of particles [34 - 38] and higher rotational frequency $\hbar\omega(I)$ [4]. Afanasjev et al. [39] studied the highly deformed bands in ^{58}Cu and also the SD bands in^{60}Zn and ^{62}Zn in the framework of Cranked relativistic mean field theory which compared with the results obtained for SD bands in ^{60}Zn and ^{61}Zn in Ref. [14].

The perturbation of the energy levels behavior clearly demonstrated in some SD bands with the increase in the spin angular momentum. This perturbation was known as staggering effects in the transition energies $\Delta I = 2$ [40]. The staggering $\Delta I = 2$ phenomenon was investigated in various Refs. [41 - 49]. Sharma et al. applied the nuclear softness formula to deduce the bandhead spin of different SD bands in the mass region A ~ 60 - 80 and to calculate the transition energies [27]. Khalaf et al. studied the properties of SD bands of mercury nuclei by using Bohr-Mottelson collective model with four unknown parameters [50]. Vidya Devi et al. used the variable moment of inertia (VMI) model to study the properties of superdeformed bands in A < 100 mass region [51]. At high spins, superdeformed rotational bands (SDRBs) are now considered as one of the most important principles in nuclear structure [52]. Many models can used to study the properties of nuclei [50,51,53]. Here, we study the properties of various isodiaphere nuclei - the nuclei in which the difference between the number of neutrons N_n and the number of protons N_p is the same - (^{40}Ca,^{58}Cu,^{60}Zn) by using the Bohr-Mottelson collective model with four and five unknown parameters. Furthermore, we aim to interpret the appeared pairing correlations in the experimental measurements for the studied nuclei.

The paper is as follows. The Bohr-Mottelson collective model with four and five unknown parameters is extended in Sec. 2.1. Also, the rotational frequency, kinematic and dynamic moments of inertia are deduced in Sec. 2.1. Section 2.2 discusses the staggering $\Delta I = 2$ phenomenon. Section 3 is devoted to the results and discussion. Finally, the conclusions are elaborated in Sec. 4.

2. Theoretical Approach

2.1. Superdeformed Rotational Band's Model (SDRB)

The rotational energy $E(I)$ of state can be calculated as a function of the spin angular momentum I of an axially symmetric deformed nucleus by using Bohr-Mottelson collective rotational model [54] with finite number of unknown parameters,

$$E(I) = X_1[I(I+1)] + X_2[I(I+1)]^2 + X_3[I(I+1)]^3 + \cdots + X_i[I(I+1)]^i, \qquad (1)$$

this can be reduced to

$$E(I) = \sum_{i=1}^{k} X_i[I(I+1)]^i \ , \qquad (2)$$

where X_i are the unknown parameters, as $i = 1,2,3,\ldots,k$ and $X_1 = \frac{\hbar^2}{2J_0}$, where J_0 is called the bandhead moment of inertia.

The gamma-ray transition energy in a band $E_\gamma(I)$ is defined as a difference between two sequence rotational energy states which is given as,

$$E_\gamma(I) = E(I) - E(I-2), \qquad (3)$$

where $E(I-2)$ reads

$$E(I-2) = \sum_{i=1}^{k} X_i[(I-1)(I-2)]^i. \qquad (4)$$

The gamma-ray transition energy in a band using SDRB with four unknown parameters can be deduced by substituting from Eqs.(2, 4) into Eq.(3) where ($k = 4$) as

$$E_\gamma(I) = X_1[4I-2] + X_2[8I^3 - 12I^2 + 12I - 4] + X_3[12I^5 - 30I^4 + 64I^3 - 66I^2 + 36I - 8] + X_4[16I^7 - 56I^6 + 184I^5 - 320I^4 + 360I^3 - 248I^2 + 96I - 16]. \quad (5)$$

While the gamma-ray transition energy in a band using SDRB with five unknown parameters can be deduced by substituting from Eqs.(2, 4) into Eq.(3) where ($k = 5$) as

$$E_\gamma(I) = X_1[4I-2] + X_2[8I^3 - 12I^2 + 12I - 4] + X_3[12I^5 - 30I^4 + 64I^3 - 66I^2 + 36I - 8] + X_4[16I^7 - 56I^6 + 184I^5 - 320I^4 + 360I^3 - 248I^2 + 96I - 16] + X_5[20I^9 - 90I^8 + 400I^7 - 980I^6 + 1684I^5 - 1970I^4 + 1560I^3 - 800I^2 + 240I - 32] \quad (6)$$

The rotational frequency $\hbar\omega$ can be deduced from the first order derivative of the γ-ray transition energy with respect to the spin angular momentum

$$\hbar\omega(I) = \frac{dE_\gamma(I)}{dI}. \quad (7)$$

Also, the kinematic $J^{(1)}$ and dynamic $J^{(2)}$ moments of inertia can be calculated from the following expressions,

$$\frac{J^{(1)}}{\hbar^2} = \left[\frac{dE_\gamma(I)}{I\,dI}\right]^{-1}, \quad (8)$$

and

$$\frac{J^{(2)}}{\hbar^2} = \left[\frac{d^2E_\gamma(I)}{dI^2}\right]^{-1}. \quad (9)$$

Experimentally, the rotational frequency $\hbar\omega$ for SD bands is given as [4]

$$\hbar\omega(I) = \frac{E_\gamma(I)+E_\gamma(I-2)}{4}, \quad (10)$$

while the kinematic $J^{(1)}$ and dynamic $J^{(2)}$ moments of inertia are given as a function of γ-ray transition energies [4],

$$J^{(1)} = \frac{2I-1}{E_\gamma(I)}, \quad (11)$$

$$J^{(2)} = \frac{4}{E_\gamma(I)-E_\gamma(I-2)}. \quad (12)$$

The changes in $J^{(2)}$ with $\hbar\omega$ have been shown to be an important signature of the active inturder orbitals which mean that $J^{(2)}$ depend on the protons and neutrons occupation of high-N inturder orbitals [46].

2.2. The staggering $\Delta I = 2$ phenomenon

An amazing phenomenon of staggering $\Delta I = 2$ can be seen in SD bands, the staggering was determined by various order derivatives of γ-ray transition energies E_γ (between two sequence levels differing by two units of spin angular momentum $\Delta I = 2$) with respect to spin angular momentum *I* as

$$\Delta^{(0)}E_\gamma(I) = E_\gamma(I), \tag{13}$$

$$\Delta^{(1)}E_\gamma(I) = \frac{1}{2}\left[E_\gamma(I) - E_\gamma(I-2)\right], \tag{14}$$

$$\Delta^{(2)}E_\gamma(I) = \frac{1}{4}\left[E_\gamma(I+2) - 2E_\gamma(I) + E_\gamma(I-2)\right], \tag{15}$$

$\Delta^{(1)}E_\gamma(I)$ and $\Delta^{(2)}E_\gamma(I)$ are calculated from the first and second derivative of the gamma-ray transition energies with respect to the spin angular momentum ***I*** [55].

The dynamic moment of inertia is related to $\Delta^{(1)}E_\gamma(I)$ by,

$$J^{(2)} = \frac{2}{\Delta^{(1)}E_\gamma(I+2)}. \tag{16}$$

We calculate the staggering parameters $S^{(n)}$, to see well the variations in the transition energies [55]

$$S^{(n)}(I) = 2^n \times \left[\Delta^{(n)}E_\gamma^{exp.}(I) - \Delta^{(n)}E_\gamma^{cal.}(I)\right]. \tag{17}$$

3. Results and Discussion

The isodiaphere - the nuclei in which the difference between the number of neutrons N_n and the number of protons N_p is the same - (^{40}Ca,^{58}Cu,^{60}Zn), we choose the nuclei in which $|N_n - N_p| = 0$ and also have only one superdeformed band.

The four and five unknown parameters of isodiaphere nuclei have been estimated by fitting the experimental gamma-ray transition energies [4] using Eqs. (5,6). The best fitting parameters

are obtained using MATLAB software. The quality of the fitting is determined by the root mean square derivation χ given by the following

$$\chi = \sqrt{\frac{1}{N}\sum_i^N \left[\frac{E_\gamma^{exp.}(I_i) - E_\gamma^{cal.}(I_i)}{\Delta E^{exp.}(I_i)}\right]^2}, \quad (18)$$

where N is the number of the data entering into the fitting procedure and $\Delta E^{exp.}(I_i)$ is the experimental error of the gamma-ray transition energies. We used the calculated γ-ray energies using the best fitting parameters to calculate the rotational frequency $\hbar\omega$, the kinematic $J^{(1)}$, and the dynamic $J^{(2)}$ moments of inertia.

Table 1. The obtained fitting parameters $X_1, X_2, X_3,$ and X_4 from the four parameters formula of Bohr-Mottelson collective model, experimental [4] $E_\gamma^{exp.}(I)$ and calculated $E_\gamma^{cal.}(I)$ lowest γ-ray transition energies, and finally, the bandhead moment of inertia for studied isodiaphere nuclei.

SD	X_1 (KeV)	X_2 (KeV)	$X_3 \times 10^{-4}$ (KeV)	$X_4 \times 10^{-7}$ (KeV)	$E_\gamma^{exp.}(I)$ (KeV)	$E_\gamma^{Cal.}(I)$ (KeV)	$J_0 \times 10^{-3}$ ($\hbar^2$ MeV^{-1})
^{40}Ca	67.3456	-0.03151	1.143	-2.62115	418	402.964	0.007424
^{58}Cu	6.34799	0.0783897	-1.11303	67.7479	830	838.791	0.078765
^{60}Zn	34.7429	-0.023529	0.261	-0.0843	1136	1157.941	0.014391

Tables 1,2 list the obtained fitting parameters X_1, X_2, X_3, X_4 and X_5 (using MATLAB software), the experimental $E_\gamma^{exp.}(I)$ and calculated $E_\gamma^{cal.}(I)$ lowest γ-ray transition energies for each SD band using Bohr-Mottelson collective rotational model [54] with four and five unknown parameters, respectively. We found that our results are in good agreement with the experimental

measurements using both Bohr-Mottelson collective rotational model [54] with four and five unknown parameters. Additionally, the bandhead moment of inertia is calculated in Tabs. (1,2) using both models.

Table 2. The obtained fitting parameters $X_1, X_2, X_3, X_4,$ and X_5 from the five parameters formula of Bohr-Mottelson collective model, experimental [4] $E_\gamma^{exp.}(I)$ and calculated $E_\gamma^{cal.}(I)$ lowest γ-ray transition energies, and finally, the bandhead moment of inertia for studied isodiaphere nuclei.

SD	X_1 (KeV)	X_2 (KeV)	$X_3 \times 10^{-4}$ (KeV)	$X_4 \times 10^{-7}$ (KeV)	$X_5 \times 10^{-10}$ (KeV)	$E_\gamma^{exp.}(I)$ (KeV)	$E_\gamma^{Cal.}(I)$ (KeV)	$J_0 \times 10^{-3}$ ($\hbar^2$ MeV^{-1})
^{40}Ca	69.9676	-0.17225	19.475	-90.1	139	418	414.014	0.007146
^{58}Cu	0.95412	0.12338	-2.79	3.52	-1.79	830	830.216	0.52404
^{60}Zn	30.1805	0.004874	-0.458	0.706	-0.313	1136	1144..684	0.016567

Figure 1 presents the experimental [4] $E_\gamma^{exp.}(I)$ and calculated $E_\gamma^{cal.}(I)$ lowest γ-ray transition energies as a function of the spin angular momentum *I* for isodiaphere nuclei (^{40}Ca,^{58}Cu,^{60}Zn). The experimental data are represented by solid circles and the calculated data using SDRB with four and five unknown parameters are represented by solid red and blue lines, respectively. We notice a good agreement between measured and calculated gamma-ray transition energies especially calculations using SDRB with five unknown parameters. Also, the calculated gamma-ray transition energies of ^{58}Cu using SDRB with five parameters agree with measured ones more than the results using the nuclear softness formula [27].

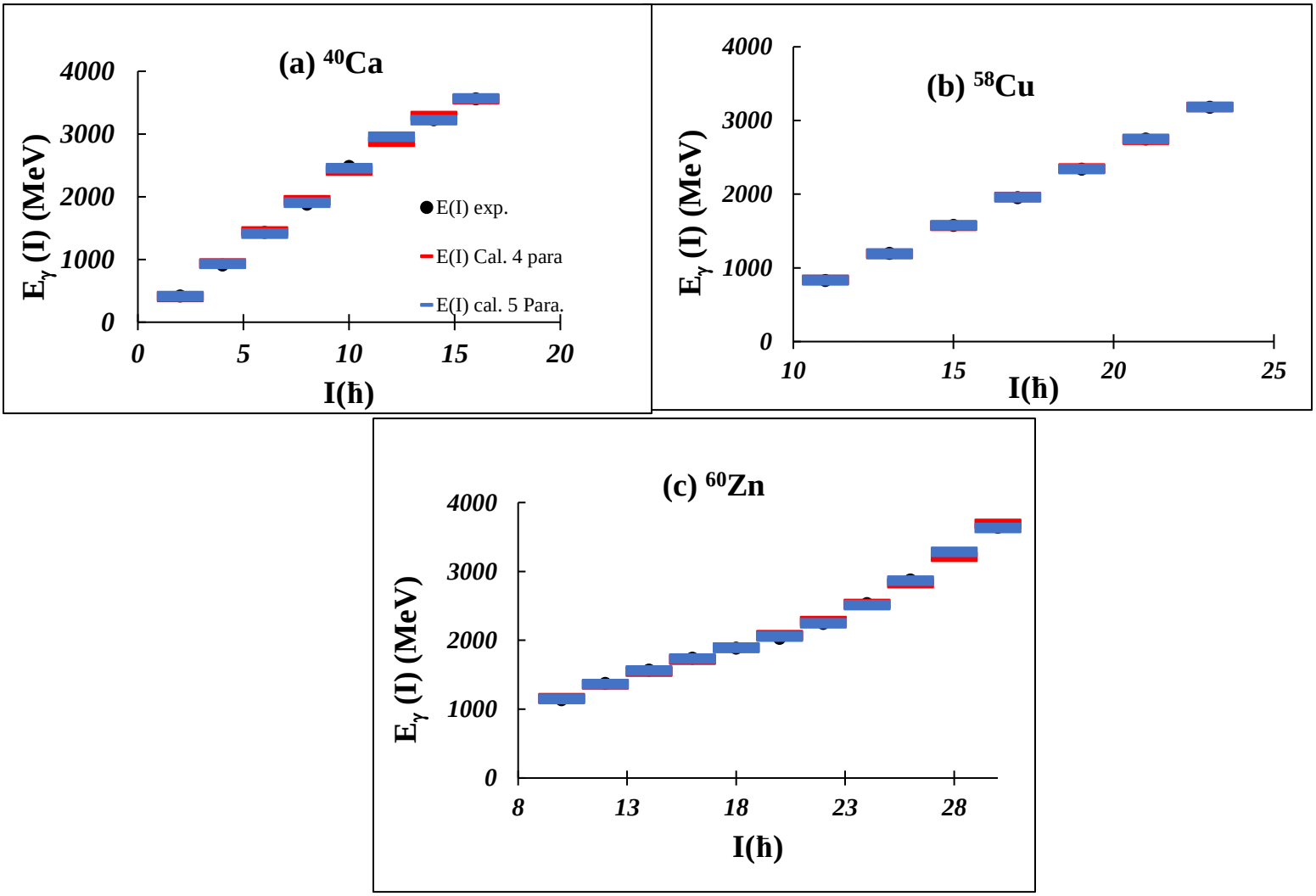

Fig. 1. [Color online] The experimental $E_{\gamma}^{exp.}(I)$ [4] and calculated $E_{\gamma}^{cal.}(I)$ lowest γ-ray transition energies as a function of the spin angular momentum I for isodiaphere nuclei (^{40}Ca,^{58}Cu,^{60}Zn).

Figure 2 presents the kinematic $J^{(1)}$ and the dynamic $J^{(2)}$ moments of inertia as a function of the rotational frequency $\hbar\omega$ for SD bands, (a) ^{40}Ca, (b) ^{58}Cu and (c) ^{60}Zn. The experimental data [4] are represented by symbols (square for $J^{(1)}$ and circle for $J^{(2)}$). The dashed and solid curves are the calculated kinematic $J^{(1)}$ moments of inertia using SDRB with four and five unknown parameters, respectively. Also, the doted and solid curves are the calculated dynamic

$J^{(2)}$ moments of inertia using SDRB with four and five unknown parameters, respectively. In all panels, we found that the results of $J^{(1)}$ using both SDRB formula agree very well with the experimental measurements.

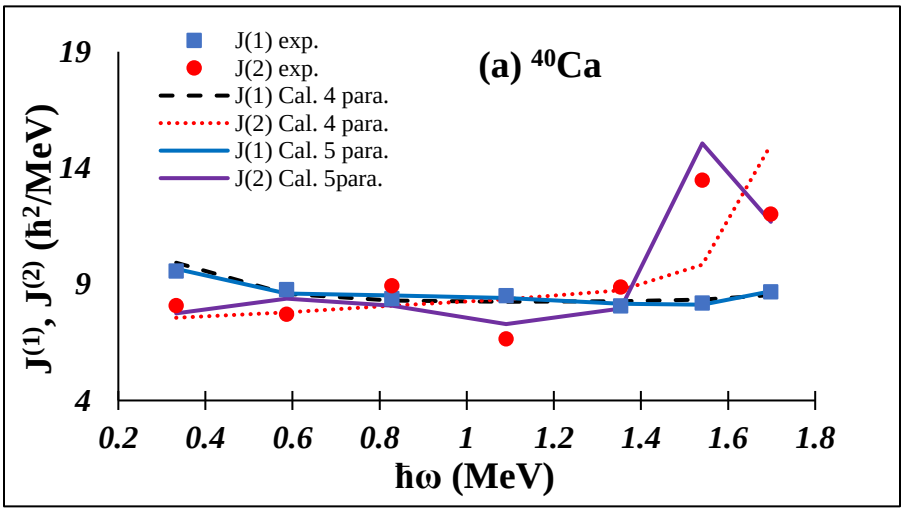

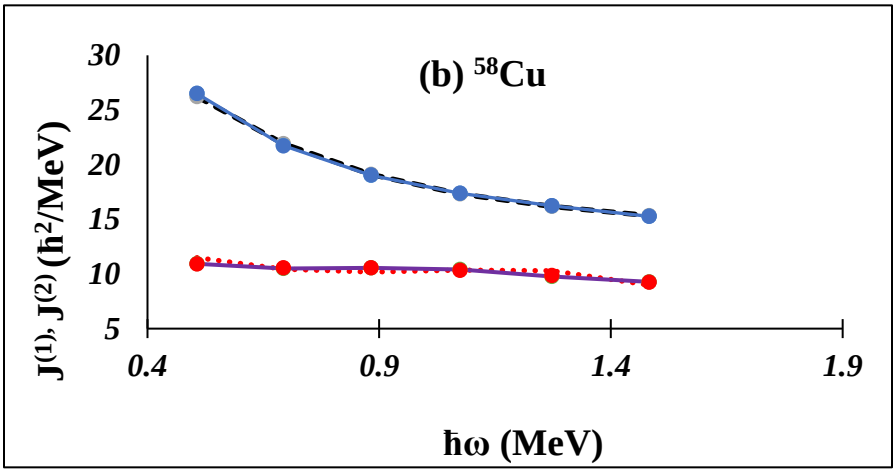

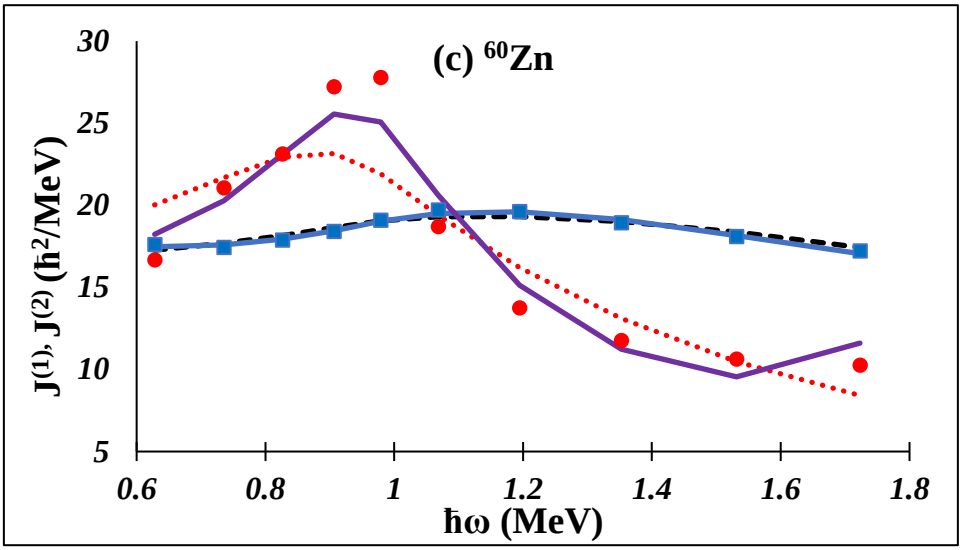

Fig. 2. [Color online] The kinematic $J^{(1)}$ and dynamic $J^{(2)}$ moments of inertia as a function of the rotational frequency $\hbar\omega$ for isodiaphere nuclei (^{40}Ca,^{58}Cu,^{60}Zn). The experimental measurements [4] are represented as symbols. The calculated results for $J^{(1)}$ and $J^{(2)}$ are given as solid and dashed curves, respectively.

Figure (2a) shows $J^{(1)}$ and $J^{(2)}$ values for SD band in ^{40}Ca as a function of $\hbar\omega$. It is noted that the calculated $J^{(1)}$ using both formulas agree well with the experimental measurements. For $J^{(2)}$ results, we found that calculations of $J^{(2)}$ using SDRB with five unknown parameters agree well with the experimental measurements more than calculations using SDRB with four unknown parameters, especially at $\hbar\omega > 1.2$. This means that Bohr-Mottelson collective model with five unknown parameters able to interpret the appeared pairing correlations - which result from the arrangements of $f_{7/2}$ protons and neutrons - in the experimental measurements.

Figure (2b) depicts the good agreement between our calculations for $J^{(1)}$ and $J^{(2)}$ with the experimental data for SD band in ^{58}Cu. $J^{(2)}$ values are found to be less than $J^{(1)}$ for all values of $\hbar\omega$ for SD band in ^{58}Cu. Both plots of $J^{(1)}$ and $J^{(2)}$ are concave downward. The variations of $J^{(2)}$ values with the increase in $\hbar\omega$ are characteristic of different high-N inturder orbitals which is due to the individual trend of occupied inturder orbitals.

Figure (2c) represents shows $J^{(1)}$ and $J^{(2)}$ values for SD band in ^{60}Zn as a function of $\hbar\omega$. Our calculations for $J^{(1)}$ agree very well with the experimental data for SD band in ^{60}Zn. For $J^{(2)}$ results, we found that calculations of $J^{(2)}$ using SDRB with five unknown parameters agree well with the experimental measurements more than calculations using SDRB with four unknown parameters especially at low $\hbar\omega$. This means that Bohr-Mottelson collective model with five unknown parameters success in interpreting the pairing correlations in the low-spin SD states. Especially, the strong upbend in $J^{(2)}$ values (both experimentally and calculated ones) at low $\hbar\omega$ - range from 0.8-1.0 MeV - which interpreted as a manifestation of the arrangements of the $g_{9/2}$ protons and neutrons. After $\hbar\omega > 1$ MeV, $J^{(2)}$ values decrease with the increase in $\hbar\omega$. Furthermore, $J^{(2)}$ values are less than $J^{(1)}$ due to the decrease in the collectivity in this band.

For the A ~ 40-60 mass region, the observed SD nuclei have a larger deformation, $\varepsilon_2 \approx 0.353 - 0.486$ and rotate most rapidly. $\hbar\omega$ is from 0.4 MeV to 1.9 MeV, and the pairing correlations have a great significant in most isodiaphere nuclei especially (^{40}Ca,^{60}Zn). The decreasing, oscillating, and strong bending behaviour of $J^{(2)}$may contribute to the alignments of the protons and neutrons (or individually in ^{58}Cu) and the appearance of pairing correlations in all (^{40}Ca,^{60}Zn).

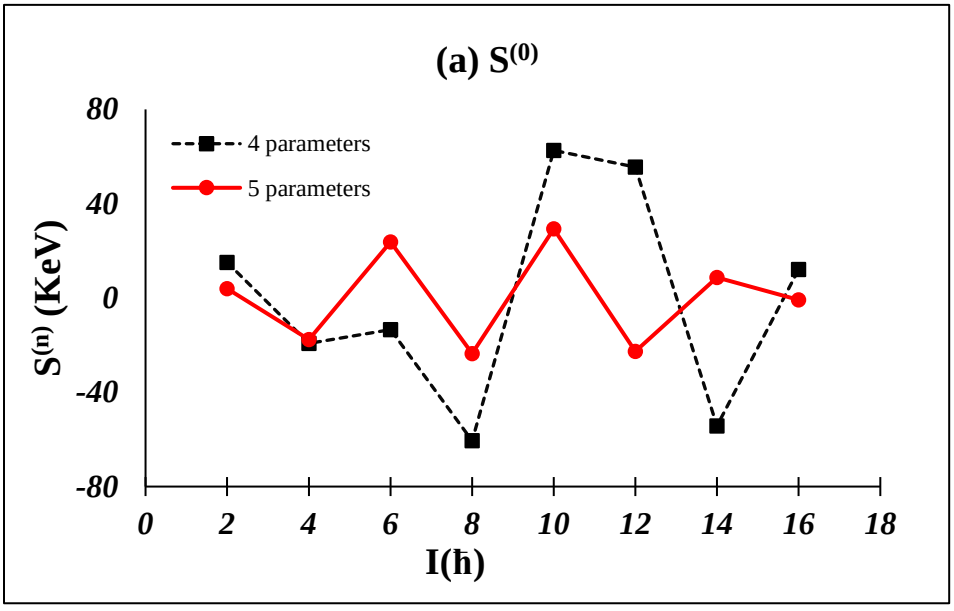

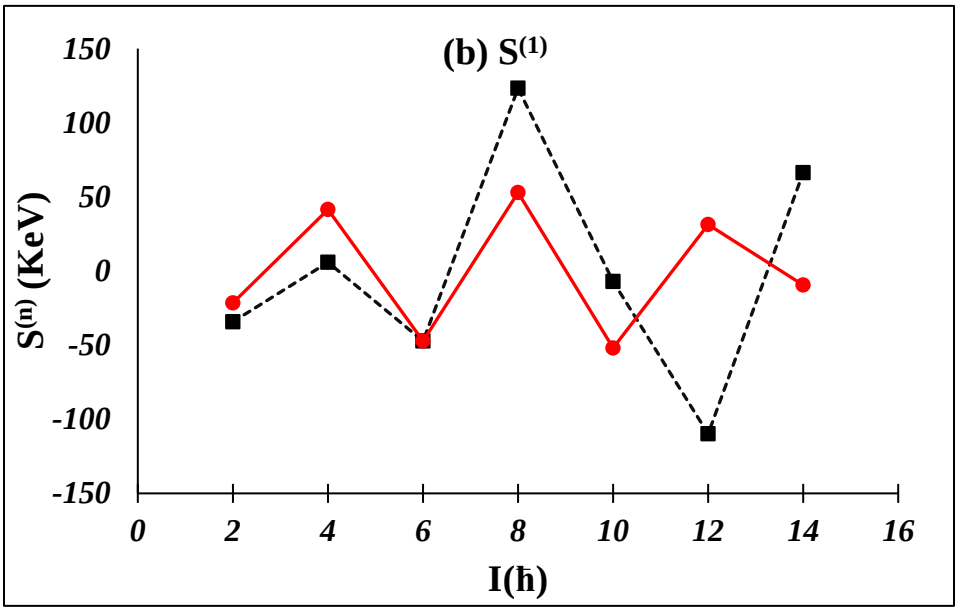

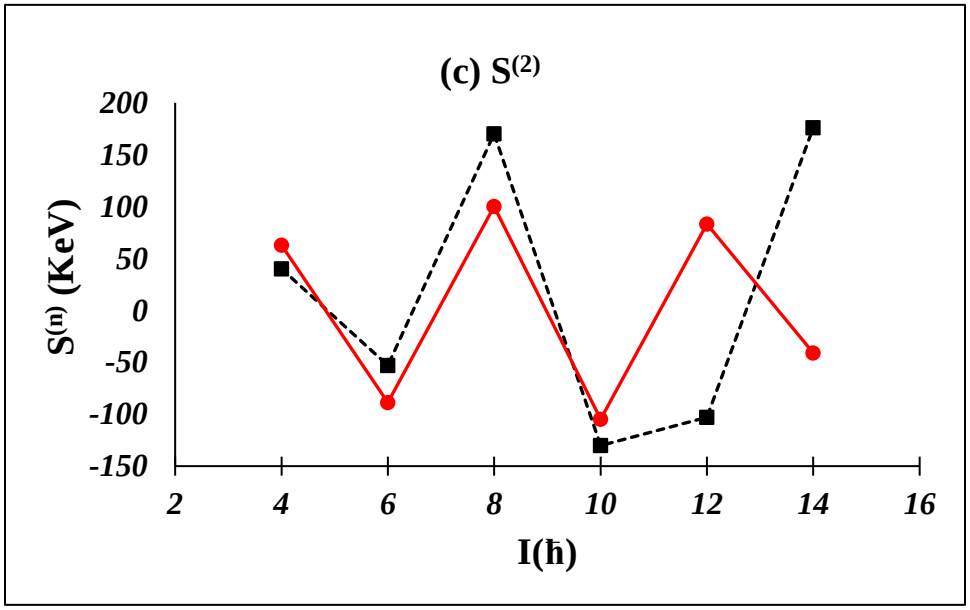

Fig. 3. The $\Delta I = 2$ staggering parameter $S^{(n)}(I)$ $(n = 0{:}\,2)$ calculated by the n-point formula (Eqs. (13-15)) as a function of the spin angular momentum I for ^{40}Ca.

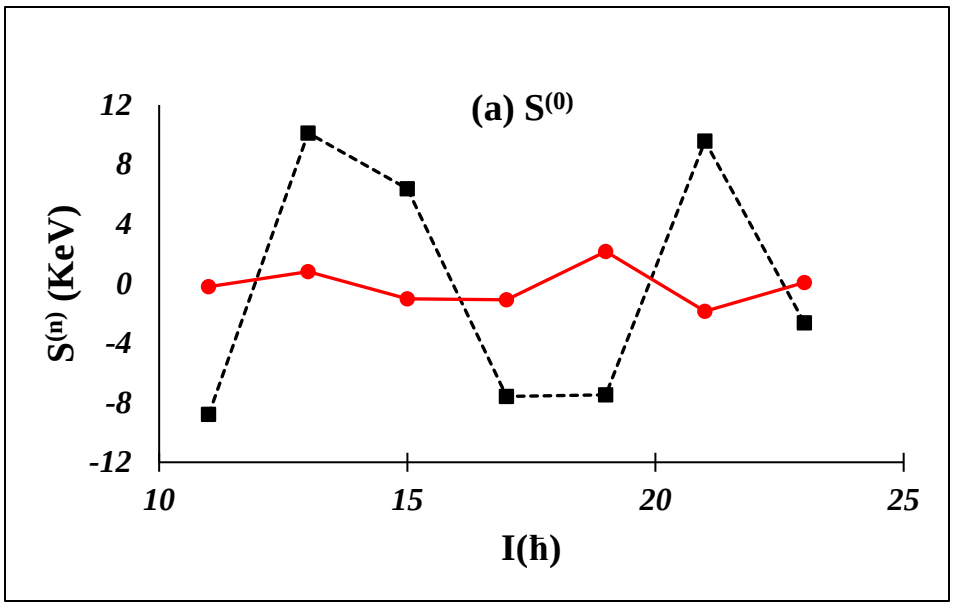
(a) S(0)
S(n) (KeV)
12
8
4
0
-4
-8
-12
10
15
20
25
I(ħ)

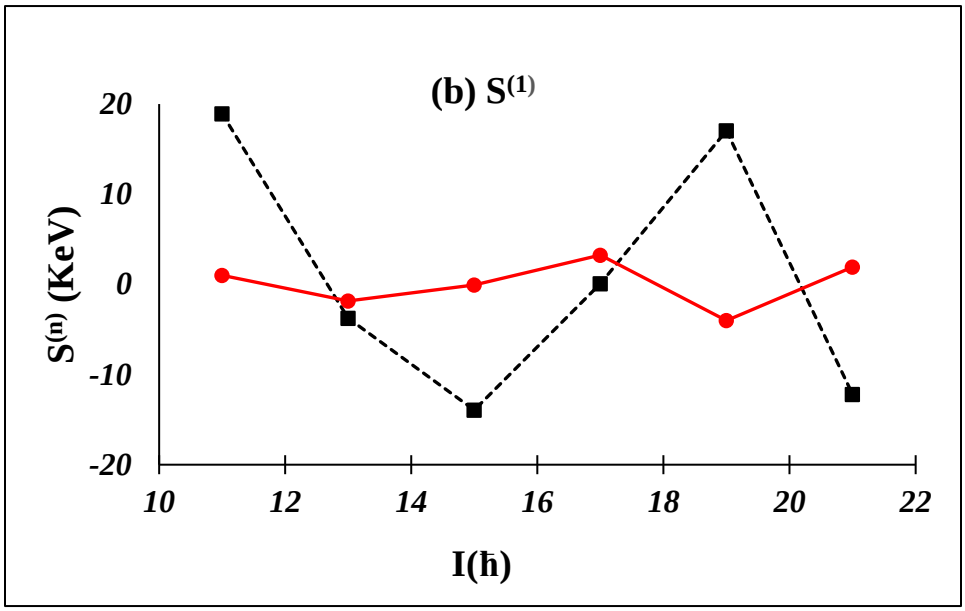
(b) S(1)
S(n) (KeV)
20
10
0
-10
-20
10
12
14
16
18
20
22
I(ħ)

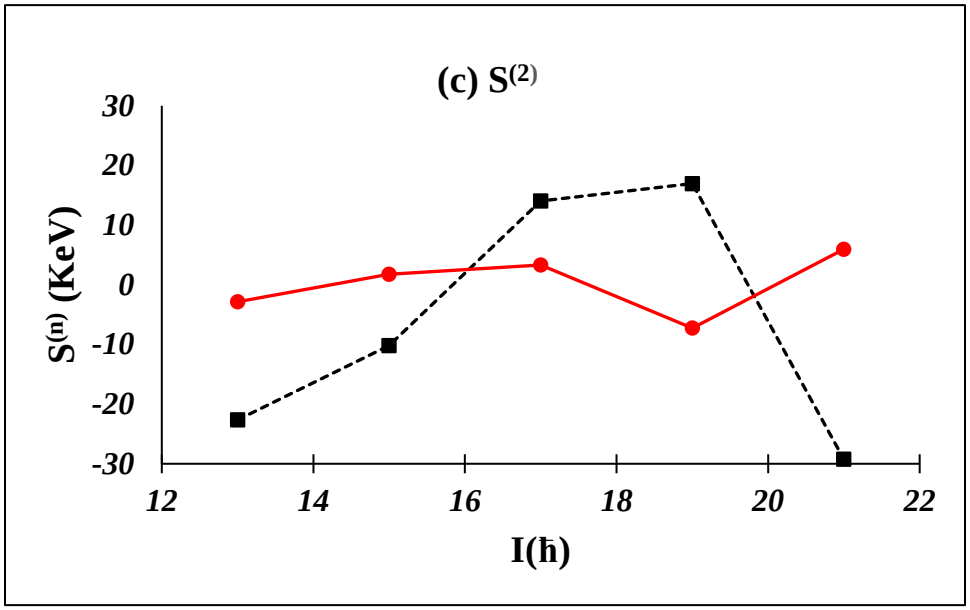

Fig. 4. The $\Delta I = 2$ staggering parameter $S^{(n)}(I)$ $(n = 0 : 2)$ calculated by the n-point formula (Eqs. (13-15)) as a function of the spin angular momentum I for ^{58}Cu.

Figures (3 - 5) show the staggering parameter $S^{(n)}(I)$ for SD bands, which is the difference between experimental and calculated ones as a function of nuclear spin angular momentum *I*. The staggering parameters calculations using SDRB with four and five unknown parameters are represented by dashed and solid lines, respectively. We notice variations in the transition energies by using the staggering parameter especially using SDRB with five unknown parameters. Changes in staggering phase result from the existence of a critical point in which the shape transition occurs. In previous, the staggering phenomena were studied using the higher-order derivatives of the gamma-ray transition energies for high mass region, here we apply the same analysis at low mass region A ~ 40 - 60.

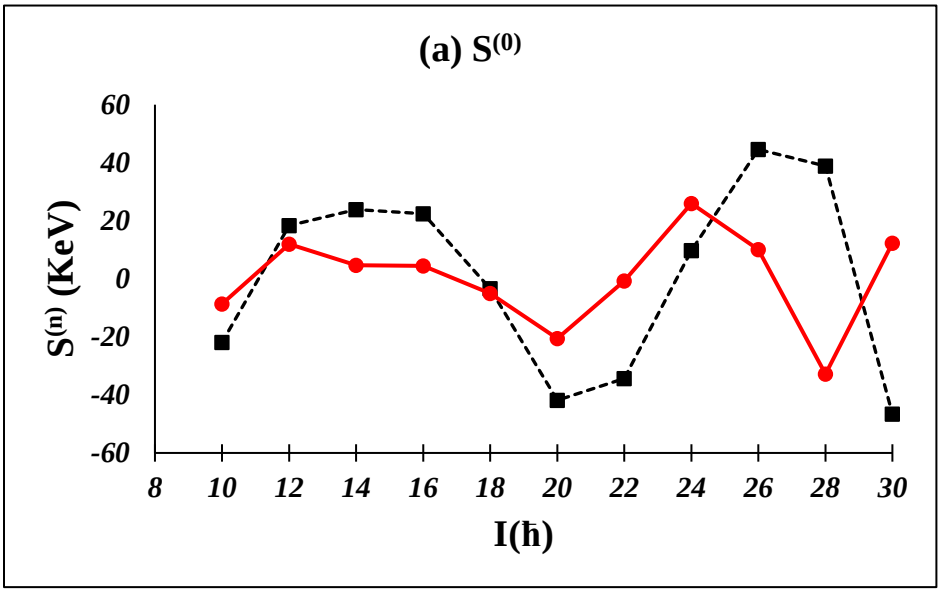
(a) S(0)
60
40
20
0
-20
-40
-60
S(n) (KeV)
8
10
12
14
16
18
20
22
24
26
28
30
I(ħ)

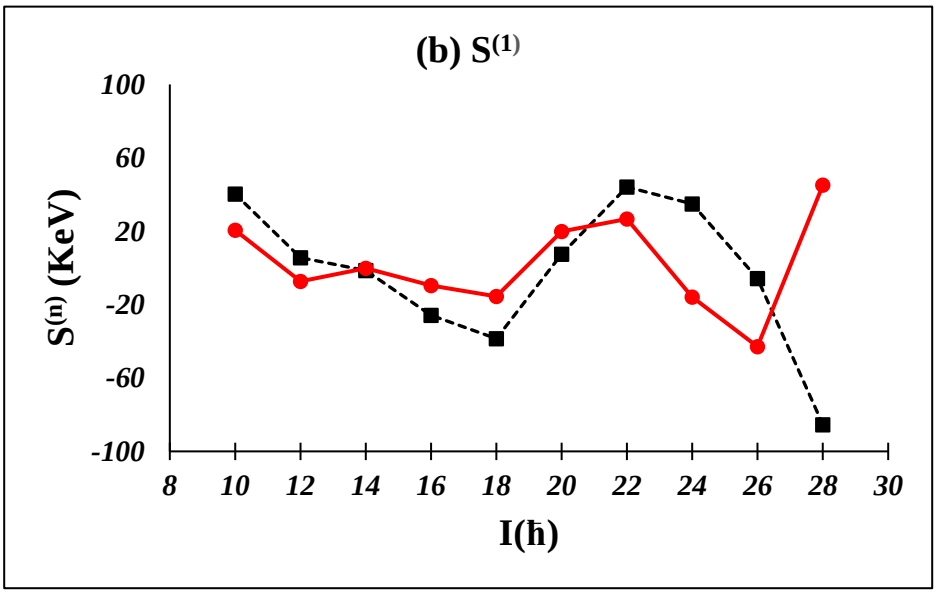
(b) S(1)
100
60
20
-20
-60
-100
S(n) (KeV)
8
10
12
14
16
18
20
22
24
26
28
30
I(ħ)

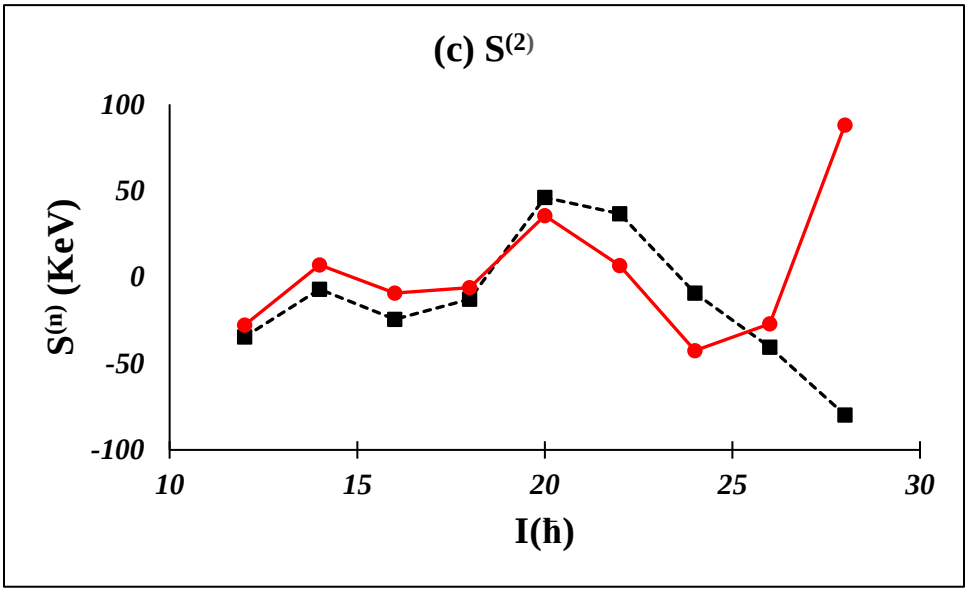

Fig. 5. The $\Delta I = 2$ staggering parameter $S^{(n)}(I)$ $(n = 0{:}\,2)$ calculated by the n-point formula (Eqs. (13-15)) as a function of the spin angular momentum I for ^{60}Zn.

4. Conclusion

The superdeformed bands of the studied isodiaphere nuclei can describe with the framework of four and five parameters' formulas of Bohr-Mottelson collective model. Both formulas give a direct relation between the energy and the spin angular momentum. Firstly, the experimental measurements of the gamma-ray transition energy for ^{40}Ca,^{58}Cu, and ^{60}Zn nuclei are fitted using the extended formulas by MATLAB software. Then, the obtained fitting parameters are used to calculate the gamma-ray transition energy for the examined nuclei in mass region A ~ 40 - 60.

The results for all studied nuclei agree well with the experimental data, especially calculations using SDRB with five unknown parameters formula. Comparing with the previous calculations for ^{58}Cu from Ref. [27], our results are more accurate than the later. Using the fitting parameters and the theoretical gamma-ray transition energy, the rotational frequency $\hbar\omega$, the kinematic $J^{(1)}$ and dynamic $J^{(2)}$ moments of inertia were calculated. Our results are in a good agreement with the experimental ones. The staggering phenomenon was examined for the studied nuclei using four and five parameters' formulas of Bohr-Mottelson collective model. We

find $\Delta I = 2$ staggering in all studied isodiaphere nuclei. Large significant staggering appears for these nuclei when calculating and plotting the staggering parameters $S^{(n)}(I)$ versus the spin angular momentum. Finally, we conclude that Bohr-Mottelson collective model with five unknown parameters successes to interpret the appeared pairing correlations in the experimental measurements.

Conflicts of Interest: The authors declare no conflict of interest.

References:

[1] A. N. Wilson, G. D. Dracoulis, A. P. Byrne, P. M. Davidson, G. J. Lane, R. M. Clark, P. Fallon, A. Görgen, A. O. Macchiavelli, and D. Ward, "Observation of a superdeformed band in ^{190}Pb", Eur. Phys. J. A 24: (2005), https://doi.org/10.1140/epja/i2005-10001-y.

[2] E.F. Moore, R. V. F. Janssens, R. R. Chasman, I. Ahmad, et al., "Observation of superdeformation in ^{191}Hg", Phys. Rev. Lett. 63: (1989), https://doi.org/10.1103/PhysRevLett.63.360.

[3] P.J. Twin, B. M. Nyakó, A. H. Nelson, J. Simpson, M. A. Bentley, et al., "Observation of a Discrete-Line Superdeformed Band up to $60\hbar$ in ^{152}Dy", Phys. Rev. Lett. 57: (1986), https://doi.org/10.1103/PhysRevLett.57.811.

[4] B. Singh, R. Zywina, and R.B. Firestone, "Table of Superdeformed Nuclear Bands and Fission Isomers: Third Edition (October 2002)", Nucl. Data Sheets 97: (2002), https://doi.org/10.1006/ndsh.2002.0018.

[5] X.L. Han and C.L. Wu, "Nuclear Superdeformation Data Tables", At. Data Tables 63: (1996), https://doi.org/10.1006/adnd.1996.0011.

[6] D. G. Sarantites, D. R. LaFosse, M. Devlin, F. Lerma, V. Q. Wood, C. Baktash, et al., "Triaxial superdeformed bands in $^{86}Zr86$", Phys. Rev. C 57: (1998), https://doi.org/10.1103/PhysRevC.57.R1.

[7] A. G. Smith, P. J. Dagnall, J. C. Lisle, D. H. Smalley, T. R. Werner, et al., "Observation of superdeformation in ^{82}Sr", Phys. Lett. B 355: (1995), https://doi.org/10.1016/0370-2693(95)00735-4.

[8] J.Q. Jin, C. Baktash, M. J. Brinkman, C. J. Gross, D. G. Sarantites, I. Y. Lee, B. Cederwall, F. Cristancho, et al., "Identification and Quadrupole-Moment Measurement of a Superdeformed Band in ^{84}Zr", Phys. Rev. Lett. 75: (1995), https://doi.org/10.1103/PhysRevLett.75.1471.

[9] C.H. Yu, C. Baktash, M. J. Brinkman, H.-Q. Jin, D. Rudolph, C. J. Gross, M. Devlin, et al., "Lifetime measurements of normally deformed and superdeformed states in ^{82}Sr", Phys. Rev. C 57: (1998), https://doi.org/10.1103/PhysRevC.57.113.

[10] C. Baktash, D. M. Cullen, J. D. Garrett, C. J. Gross, N. R. Johnson, W. Nazarewicz, D. G. Sarantites, J. Simpson, et al., "First Observation of a Superdeformed Band in the $N, Z \approx 40$ Mass Region", Phys. Rev. Lett. 74: (1995), https://doi.org/10.1103/PhysRevLett.74.1946.

[11] D. R. LaFosse, M. Devlin, M. Korolija, F. Lerma, D. G. Sarantites, Y. A. Akovali, et al., "Interband Transitions between Superdeformed Bands in ^{87}Nb: Evidence for a Superintruder Orbital", Phys. Rev. Lett. 78: (1997), https://doi.org/10.1103/PhysRevLett.78.614.

[12] C. E. Svensson, C. Baktash, J. A. Cameron, M. Devlin, J. Eberth, S. Flibotte, et al., "Observation and Quadrupole-Moment Measurement of the First Superdeformed Band in the $A\sim60$ Mass Region", Phys. Rev. Lett. 79: (1997), https://doi.org/10.1103/PhysRevLett.79.1233.

[13] C. E. Svensson, D. Rudolph, C. Baktash, M. A. Bentley, J. A. Cameron, M. P. Carpenter, et al., "Decay Out of the Doubly Magic Superdeformed Band in the N= Z Nucleus ^{60}Zn", Phys. Rev. Lett. 82: (1999), https://doi.org/10.1103/PhysRevLett.82.3400.

[14] C. H. Yu, C. Baktash, J. Dobaczewski, J. A. Cameron, C. Chitu, M. Devlin, et al., "Comparison of superdeformed bands in ^{61}Zn and ^{60}Zn: Possible evidence for T = 0 pairing", Phys. Rev. C 60: (1999), https://doi.org/10.1103/PhysRevC.60.031305.

[15] D. Rudolph, C. Baktash, M. J. Brinkman, E. Caurier, D. Dean, et al., "Rotational Bands in the Doubly Magic Nucleus ^{56}Ni", Phys. Rev. Lett. 82: (1999), https://doi.org/10.1103/PhysRevLett.82.3763.

[16] C. E. Svensson, A. O. Macchiavelli, A. Juodagalvis, A. Poves, I. Ragnarsson, S. Åberg, et al., "Superdeformation in the N= Z Nucleus ^{36}Ar: Experimental, deformed mean field, and spherical shell model descriptions.", Phys. Rev. Lett. 85: (2000), ... & Yu, C. H. (2000), https://doi.org/10.1103/PhysRevLett.85.2693

[17] C. E. Svensson, A. O. Macchiavelli, A. Juodagalvis, A. Poves, I. Ragnarsson, S. Åberg, et al., "Collective rotational motion in the N= Z nucleus ^{36}Ar", Nucl. Phys. A 682: (2001), 1c-11c.

[18] E. Ideguchi, D. G. Sarantites, W. Reviol, A. V. Afanasjev, M. Devlin, C. Baktash, et al., "Superdeformation in the Doubly Magic Nucleus $^{40}_{20}Ca_{20}$", Phys. Rev. Lett. 87: (2001), https://doi.org/10.1103/PhysRevLett.87.222501.

[19] W. J. Gerace and A .M. Green, "The effect of deformed states in the Ca isotopes", Nucl. Phys. A 93: (1967), https://doi.org/10.1016/0375-9474(67)90174-1.

[20] W. J. Gerace and A. M. Green, "K-band mixing and 8p-8h states in ^{40}Ca", Nucl. Phys. A 123: (1969). https://doi.org/10.1016/0375-9474(69)90498-9.

[21] A. M. Khalaf, M. M. Taha, and A. M. Ismail, "Application of Suggested Three Parameters Collective Rotational Model to Superdeformed Thallium Odd-Mass Nuclei", J. Phys.: Conf. Ser. 2304: (2022), https://doi.org/10.1088/1742-6596/2304/1/012014.

[22] A. M. Khalaf, K. E. Abdelmageed, and E. Saber, "Description of Superdeformed Bands of Odd-A and Odd-Odd Mercury and Thallium Nuclei", Int. J. Theor. Appl. Sci. 6: (2014), 47.

[23] J. A. Becker, E. A. Henry, A. Kuhnert, T. F. Wang, S. W. Yates, et al., "Level spin for superdeformed nuclei near A= 194", Phys. Rev. C 46: (1992), https://doi.org/10.1103/PhysRevC.46.889.

[24] J. Y. Zeng, J. Meng, C. S. Wu, E. G. Zhao, Z. Xing, et al., "Spin determination and quantized alignment in the superdeformed bands in ^{152}Dy, ^{151}Tb, and ^{150}Gd", Phys. Rev. C 44: (1991), https://doi.org/10.1103/PhysRevC.44.R1745.

[25] R. Iepenbring and K.V. Protasov, "Model of superfluid liquid with triplet pairing, cranking model and model of variable moment of inertia in superdeformed bands in A∼ 190 region", Z. Phys. A 345: (1993), https://doi.org/10.1007/BF01290333.

[26] F. R. Xu and J. M. Hu, "Cranking Bohr-Mottelson Hamiltonian applied to superdeformed bands in A∼ 190 region", Phys. Rev. C 49: (1994), https://doi.org/10.1103/PhysRevC.49.1449.

[27] H. Sharma and H. M. Mittal, "Band head spin assignment of superdeformed bands in A∼ 60− 80 mass region through nuclear softness formula", Int. J. Mod. Phys. E 26: (2017), https://doi.org/10.1142/S0218301317500744.

[28] J. A. Becker, N. Roy, E. A. Henry, S. W. Yates, A. Kuhnert, J. E. Draper, et al., "Level spin and moments of inertia in superdeformed nuclei near A= 194", Nucl. Phys. A 520: (1990), https://doi.org/10.1016/0375-9474(90)91146-I.

[29] J. E. Draper, F. S. Stephens, M. A. Deleplanque, W. Korten, R. M. Diamond, W. H. Kelly, et al., "Spins in superdeformed bands in the mass 190 region", Phys. Rev. C 42: (1990), https://doi.org/10.1103/PhysRevC.42.R1791.

[30] X. T. He, S. X. Liu, S. Y. Yu, J. Y. Zeng, et al., "The $i_{13/2}$ proton intruder orbital and the identical superdeformed bands in $^{193,194,195}Tl$", Eur. Phys. J. A 23: (2005), https://doi.org/10.1140/epja/i2004-10092-x.

[31] A. M. Khalaf, M. A. Allam, and M. M. Sirag, "Bandhead Spin Determination and Moments of Inertia of Superdeformed Nuclei in Mass Region 60-90 Using Variable Moment of Inertia Model", Egypt. J. Phys. 41: (2010), 151-165.

[32] A.M. Khalaf, M.M. Sirag, and M. Taha, "Spin assignment and behavior of superdeformed bands in A~ 150 mass region", Turk. J. Phys. 37: (2013), https://doi.org/10.3906/fiz-1201-6.

[33] A.M. Khalaf, M. Kotb, Asmaa AbdElSalam and G. S. M. Ahmed, "Structure properties of yrast superdeformed bands in the mass region around gd-144", Int. J. Theor. Appl. Sci. 7(2): (2015), 33-41.

[34] R. B. Piercey, J. H. Hamilton, R. Soundranayagam, A. V. Ramayya, C. F. Maguire, et al., "Evidence for deformed ground states in light Kr isotopes", Phys. Rev. Lett. 47: (1981), https://doi.org/10.1103/PhysRevLett.47.1514.

[35] B. Cederwall, T. Bäck, R. Wyss, A. Johnson, J. Cederkäll, M. Devlin, et al., "Favoured superdeformed states in ^{89}Tc", Eur. Phys J. A 6: (1999), https://doi.org/10.1007/s100500050343.

[36] T. Back, B. Cederwall, R. Wyss, A. Johnson, J. Cederkäll, M. Devlin, et al., "Observation of superdeformed states in ^{88}Mo", Eur. Phys J. A6: (1999), https://doi.org/10.1007/s100500050361.

[37] E. ElSaady, M. ElAshmawy, H. Abu-Zeid, A. Nada, and F. Ragab, "Characterization of photo-neutrons produced by 150 MeV and 1 GeV electrons impinging on high Z-metallic targets for neutron resonance spectroscopy", J. Sci. Res. Sci., 34: (2017), https://doi.org/10.21608/jsrs.2018.14109.

[38] M. Tawfeek, W. El-Gammal, H. Abu-Zeid, A. Nada, Z. Hassan, and F. Ragab, "Characterization of Pu-bearing materials by non-destructive spectrometric approach: relevance for nuclear forensics", J. Sci. Res. Sci. (2022), https://doi.org/10.21608/jsrs.2020.44128.1033.

[39] A.V. Afanasjev, I. Ragnarsson, and P. Ring, "Comparative study of superdeformed and highly deformed bands in the A∼ 60 mass region", Phys. Rev. C 59: (1999), https://doi.org/10.1103/PhysRevC.59.3166.

[40] A.M. Khalaf, M. Kotb, and T. Awwad, "Nature of cross-talk transitions and ΔI =1 energy staggering in signature partners of odd mass superdeformed nuclei", Int. J. Mod. Phys. E 26: (2017), https://doi.org/10.1142/S0218301317500112.

[41] I. Hamamoto and B. Mottleson, "Superdeformed rotational bands in the presence of Y_{44} deformation", Phys. Lett. B 333: (1995), https://doi.org/10.1016/0370-2693(94)90144-9.

[42] L. M. Pavlichenkov and S. Flibotte, "C_4 symmetry and bifurcation in superdeformed bands", Phys. Rev. C 51: (1995), https://doi.org/10.1103/PhysRevC.51.R460.

[43] A. O. Macchiovelli, B. Cederwall, R. M. Clark, M. A. Deleplanque, et al., "C_4 symmetry effects in nuclear rotational motion", Phys. Rev. C 51: (1995), https://link.aps.org/doi/10.1103/PhysRevC.51.R1.

[44] L. A. Wu and H. Toki, "Δ I= 4 Bifurcation in Ground Bands of Even-Even Nuclei and the Interacting Boson Model", Phys. Rev. Lett. 79: (1997), https://doi.org/10.1103/PhysRevLett.79.2006.

[45] A.M. Khalaf and M.M. Sirag, "Analysis of ΔI = 2 Staggering in Nuclear Superdeformed Rotational Bands", Egypt. J. Phys. 35: (2006), 359-375.

[46] A.M. Khalaf, M.M. Taha, and M. Kotb, ", Identical Bands and ΔI = 2 Staggering in superdeformed Nuclei in A ≈150 Mass Region using Three Parameters Rotational Model", Prog. Phys. 4: (2012), 39-43.

[47] S. Flibotte, H. R. Andrews, G. C. Ball, C. W. Beausang, F. A. Beck, G. Belier, et al., "ΔI= 4 bifurcation in a superdeformed band: Evidence for a C_4 symmetry", Phys. Rev. Lett. 71: (1993), https://doi.org/10.1103/PhysRevLett.71.4299.

[48] B. Cederwall, R. V. F. Janssens, M. J. Brinkman, I. Y. Lee, I. Ahmad, et al., "New features of superdeformed bands in ^{194}Hg", Phys. Rev. Lett. 72: (1994), https://doi.org/10.1103/PhysRevLett.72.3150.

[49] A. M. Khalaf and M. D. Okashe, "Properties of nuclear superdeformed rotational bands in A~ 190 mass region", Prog. Phys. 10: (2014), 246.

[50] A.M. Khalaf, H. Yassin, and E.R. Abo Elyazeed, "Properties of signature partner superdeformed bands in mercury nuclei", J. Adv. Phys. 11: (2015), 2918.

[51] V. Devi and J. S. Matharu, "Properties of superdeformed bands in A < 100 mass region within the variable moment of inertia model", Phys. Scr. 96: (2021), https://doi.org/10.1088/1402-4896/abf18c.

[52] M. Aziz , M. D. Okasha, and G. S. M. Ahmed, "The behavior of moments of inertia and energy staggering in superdeformed nuclei", Al-Azhar Bulletin of Science: Section B 32: (2021), 7-14.

[53] A. Makram-Allah, M. Ahmed, D. Abo-Kahla, "The interaction between a Three-Level Atom and Four Systems of N-Two Level Atoms", J. Sci. Res. Sci. 37: (2020), https://doi.org/10.21608/jsrs.2020.129796.

[54] A. Bohr and Mottelson, Nuclear Structure, volume 2, Benjamin, New York, 1975.

[55] A. M. Khalaf, M. M. Sirag, and M. Kotb, "Energy Staggering in Ground Bands of ^{232}Th and $^{236,238}U$ Nuclei Using the Interacting Vector Boson Model", Commun. Theor. Phys. 64: (2015), https://doi.org/10.1088/0253-6102/64/1/90.

الملخص العربى

التعرج فى النطاقات فائقة التشوه لانوية الغلاف المتساوى ذات العدد الكتلى يتراوح من 40 ل 60

إيمان رضا ابو اليزيد ، هاجر هشام سعودى ، دعاء على معتمد الريان ، هيام يسن سيد

قسم الفيزياء ، كلية البنات للآداب والعلوم والتربية ، جامعة عين شمس ، 11577 القاهرة ، مصر

الملخص العربى

قد تم تحليل خصائص النطاقات فائقة التشوه (SD) لأنوية الغلاف المتساوى (isodiaphere) ($^{40}Ca,^{58}Cu,^{60}Zn$) بشكل منهجى فى إطار صيغ رباعية وخماسية المعاملات لنموذج بوهر- موتلسون الجماعي. تم الحصول على هذه المعاملات الغير معروفة من خلال التوفيق بين القيم النظرية والمعملية لطاقات الجاما الانتقالية باستخدام برنامج MATLAB. وقد استخدمت أفضل المعاملات المجهزة والمنتقاة لحساب طاقات الجاما الانتقالية E_γ والترددات الدورانية $\hbar\omega$ ، عزم القصور الذاتى الحركي $J^{(1)}$و عزم القصور الذاتى الديناميكي $J^{(2)}$. طاقات انتقال اشعة جاما التي تم الحصول عليها $E\gamma$ متوافقة جيدًا مع القياسات التجريبية. وأيضًا ، النتائج النظرية لعزم القصور الذاتى الحركي $J^{(1)}$ و عزم القصور الذاتى الديناميكي $J^{(2)}$ باستخدام كلا الصيغتين تتفق جيدًا مع البيانات التجريبية. وقد تم تمثيل ظاهرة سلوك التعرج $\Delta I = 2$ المذهلة باستخدام مشتقات ترتيب مختلفة لطاقات انتقال $E\gamma$ بالنسبة للزخم الزاوي الدوراني I. نستنتج أن صيغة المعاملات الخمسة لنموذج بوهر -موتلسون الجماعي تنجح في تفسير ارتباطات الاقتران الظاهرة في القياسات التجريبية للأنوية قيد الدراسة.